

Investigation of the Sequence Distribution of Bulk and Emulsion Styrene–Acrylic Acid Copolymers by ^1H - and ^{13}C -NMR

SHOUTING WANG and GARY W. POEHLIN*

School of Chemical Engineering, Georgia Institute of Technology, Atlanta, Georgia 30332-0370

SYNOPSIS

The sequence distribution of homogeneous styrene (S)–acrylic acid (A) copolymers, obtained by low conversion (< 10%) bulk copolymerization, has been studied by ^1H - and ^{13}C -NMR. The reactivity ratios r_a and r_s were determined by the Kelen–Tudos method. The sequence distributions at the triad level were assigned and verified by Alfrey–Mayo kinetics. The sequence distributions of emulsion copolymers formed at different reaction conversions were investigated and compared with the results obtained from bulk copolymers. © 1993 John Wiley & Sons, Inc.

INTRODUCTION

Functional monomers are sometimes used^{1–5} to increase stabilization of latex particles during polymerization and in post-polymerization processes, such as residual monomer stripping, formulation, storage, shipping, and application. Functional monomers are also used to enhance affinity performance such as adhesion improvement. These functional monomers are generally highly soluble in water. Some of the important questions concerning such comonomers are: How do the functional monomer units in copolymers act as stabilizing agents for the polymer particles? How and where are they incorporated into the latex particles? How do they contribute to the hydrophilic–hydrophobic balance of the surface of the latex particles?

In order to address these questions, the copolymerization behavior of functional monomers in the emulsion system and the structure of copolymer containing functional monomers needs to be more completely understood. Emulsion copolymerization kinetics of some water-soluble functional monomers and the partition of these monomers in emulsion copolymerization systems have been studied in this

laboratory.^{6–8} Experimental studies of the intramolecular microstructure (triad distribution) of bulk and emulsion copolymers containing functional monomers are presented in this paper.

Nuclear magnetic resonance (NMR) spectroscopy has been established as a primary technique for the microstructure analysis of copolymers.^{9–13} The microstructure of homopolymer, that is, end groups and tacticity, has been analyzed by NMR.¹³ NMR techniques have been widely used to study copolymer composition and monomer sequence distribution. In the 1960s, Bovey used a statistical method to assign the sequence distribution of methyl methacrylate–styrene (MMA-S) and MMA- α -methylstyrene (MMA- α -MS) copolymers from ^1H -NMR data.¹⁴ Ito et al. studied the coisotacticity of MMA-S,¹⁵ MMA- α -MS,¹⁶ MMA-methyl acrylate (MMA-MA),¹⁷ and vinylidene chloride–vinyl acetate (VC-VA)¹⁸ copolymers by ^1H -NMR.

In the 1970s and 1980s, ^{13}C -NMR has been used to investigate a number of polymer systems with generally excellent results. The large chemical shift range in ^{13}C -NMR permits the study of more complex copolymer systems and the elucidation of detailed structural information.^{19–25} Uebel et al., for example, reassigned the sequence distribution of MMA-S copolymer and determined the reactivity ratios of butylstyrene–MMA copolymerization.^{26,27} Brar et al. assigned the sequence distribution of

* To whom correspondence should be addressed.

Table I Monomer Feed and Composition of S-AA Bulk Copolymers^a

Sample Code ^b	Mole Fraction of Styrene in Feed	Conversion of Reaction (%)	Average Mole Fractions of Styrene in Copolymers ^c
SA-5	0.929	1.4	0.856
SA-10	0.863	0.6	0.772
SA-20	0.735	2.4	0.673
SA-30	0.618	2.9	0.638
SA-40	0.509	4.2	0.586
SA-50	0.410	5.0	0.555
SA-60	0.316	5.5	0.520
SA-80	0.148	8.7	0.344

* Initiator was AIBN at 1 wt % of total monomers.

^b The numbers are the wt % of AA in feed.

^c Determined by NMR.

MMA-ethyl methacrylate (MMA-EMA), MMA-S, MMA-*n*-butyl methacrylate (MMA-*n*-BuMA), and acrylic acid-MMA (AA-MMA) copolymers by ¹³C-NMR.²⁸⁻³¹ Tacx et al. investigated solution and emulsion copolymers of S-EMA and S-MA and proposed a microstructure model for high conversion copolymerization.³²⁻³⁴ Recently the monomer sequence distributions of chlorotrifluoroethylene-vinyl acetate (CTFE-VA) and CTFE-vinyl propionate

emulsion copolymers were determined.³⁵ The development of two-dimensional NMR spectroscopy permits easier assignment of complex copolymer spectra peaks.³⁴

Most copolymer sequence distribution studies have involved copolymers of ester monomers with other hydrophobic monomers in which the chemical shifts of the ester group are very sensitive to the microstructure. One question concerning the monomer system of styrene-acrylic acid (S-AA) is whether sequence distribution information can be determined in NMR spectra. In this work, ¹H- and ¹³C-NMR spectra of S-AA copolymers were examined to determine the resonances that are sensitive to the copolymer microstructure. The compositions of the copolymers were measured by NMR and the reactivity ratios calculated. Finally, the triad sequences were assigned by experiments and the Alfrey-Mayo (AM) statistics-kinetics model.

EXPERIMENTAL

Acrylic acid and styrene (Aldrich) were distilled at reduced pressure under nitrogen. The middle fraction of the distillate was stored in a refrigerator until use. The free-radical initiator AIBN (Kodak) was recrystallized once from methanol. Potassium persulfate (Fair Lawn), sodium dodecyl sulphate

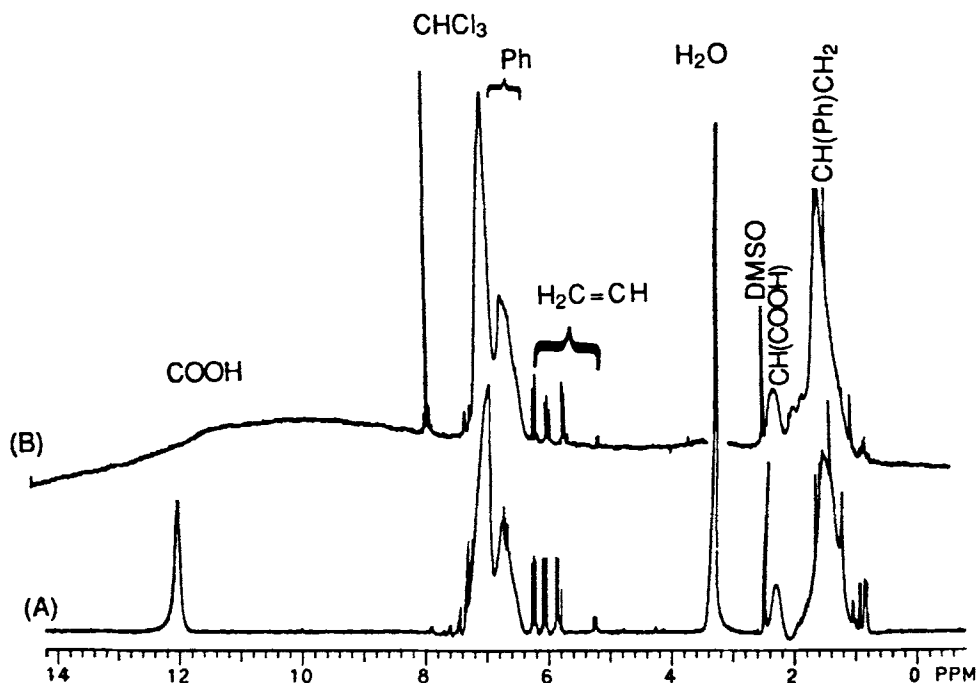


Figure 1 ¹H-NMR spectra of styrene and acrylic acid copolymer, SA-40, (A) DMSO-D₆ and (B) DMSO-D₆-CDCl₃ solvent mixture at 50°C.

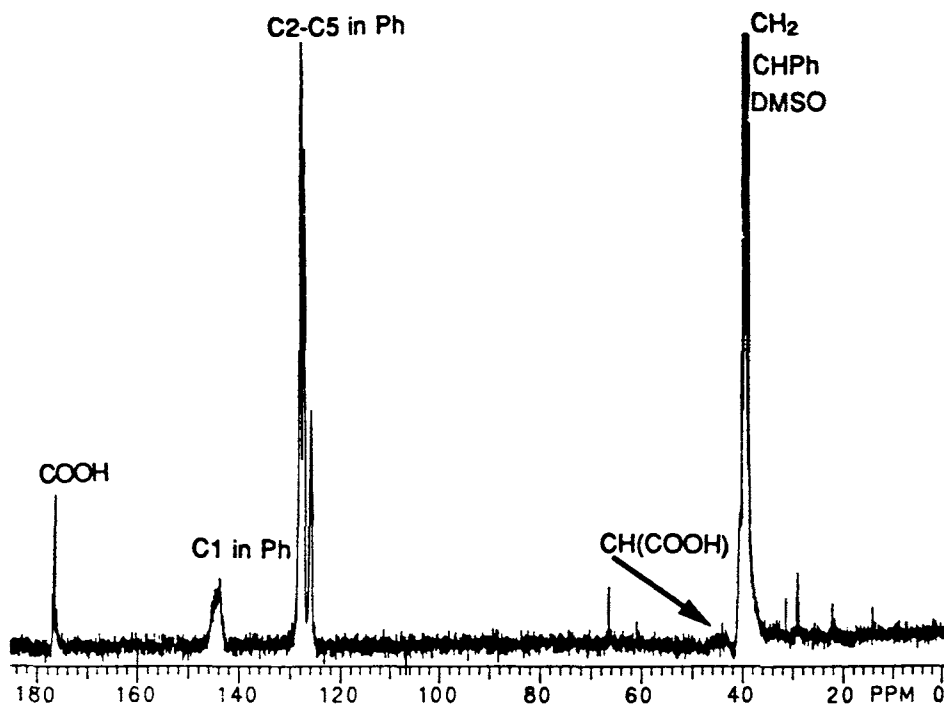


Figure 2 ^{13}C -NMR spectra of styrene-acrylic acid copolymer, SA-40, DMSO as solvent at 90°C .

(BDH, England), and hydroquinone (Fisher) were used as received. The water was deionized.

Bulk copolymerizations were carried out at 50°C in a 250 mL three-neck flask equipped with a reflux condenser, a glass stirrer, and nitrogen inlet tube. The polymerization recipes are shown in Table I. The reaction was started by rapidly heating 50 g of

monomer mixture and 0.5 g AIBN in an agitated reactor under a nitrogen atmosphere. The total conversion was determined gravimetrically. The copolymer was isolated by pouring samples of the reaction mixture into a 15-fold excess of iso-octane. The final products were dried in air and then at 65°C in a vacuum oven for 48 h.

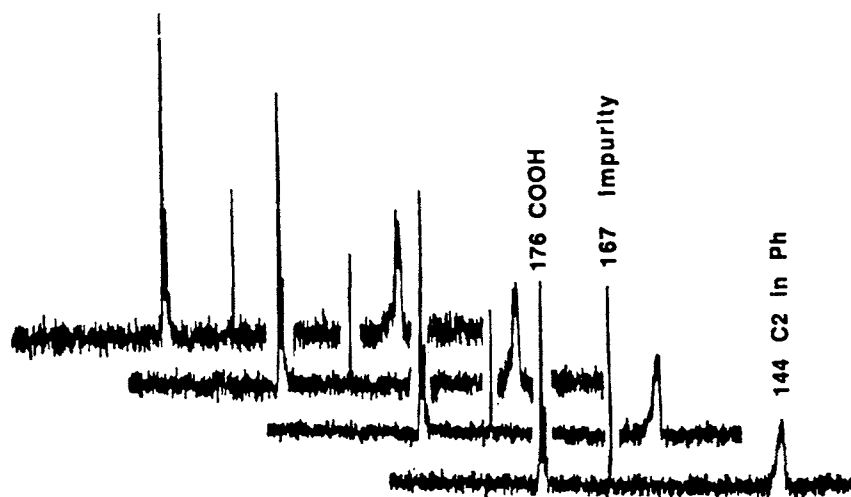


Figure 3 ^{13}C -NMR spectra of selected carbon atoms in styrene-acrylic acid copolymer at different temperatures. Temperature: 30, 50, 70, and 90°C from bottom to top spectra; Solvent: DMSO-D_6 .

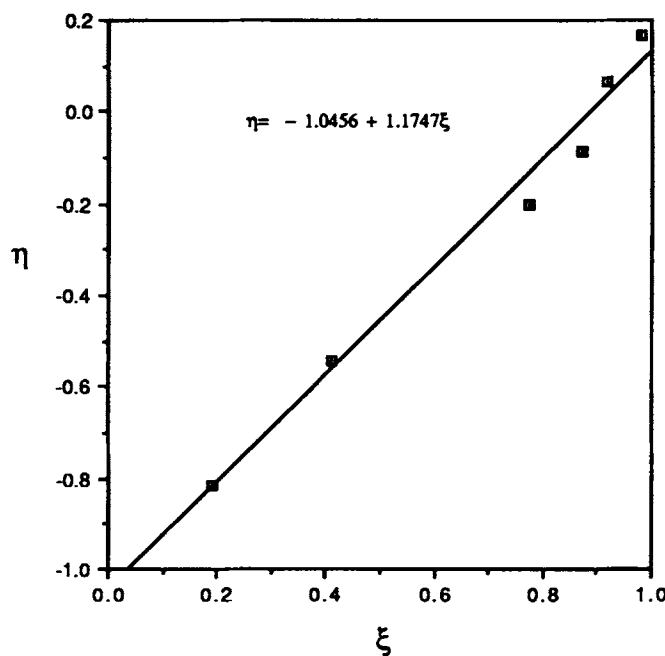
Table II Fraction of Styrene in Initial Monomer Feed (f_s) and in Bulk Copolymers (F_S) Obtained by ^1H - and ^{13}C -NMR

Sample Code	f_s	^1H -NMR		^{13}C -NMR	
		F_{S-1}	F_{S-2}	F_{S-3}	F_{S-4}
SA-5	0.929		0.8473	0.8651	
SA-10	0.863		0.7686	0.7647	0.7832
SA-20	0.735		0.6865	0.6568	0.6742
SA-30	0.618		0.6598	0.6254	0.6378
SA-40	0.509	0.5312	0.5797	0.5715	0.6080
SA-50	0.410	0.5384	0.5483	0.5401	0.5780
SA-60	0.316	0.4629	0.5311	0.4973	0.5329
SA-80	0.148	0.3342	0.3331	0.3479	0.3515

The emulsion polymers were prepared in a 1-L stirred reactor. Monomer mixture (200 g) was pre-emulsified by addition to the soap solution (4.3 g SDS in 300 mL water) and heated to 50°C. Subsequently, the initiator solution (1 g $\text{K}_2\text{S}_2\text{O}_8$ in 40 mL water) was injected into the reactor. The reaction was stopped by mixing the samples into a hydroquinone solution (0.1 g hydroquinone in 2 mL water) and chilling with dry ice.

The measurement of NMR spectra of S-AA copolymers was complicated because of the difficulties in dissolving the samples. Copolymers with high AA content cannot be dissolved in CDCl_3 . If the styrene

content is high, the copolymer cannot be dissolved by DMSO-D_6 . Hence the NMR spectra were recorded using DMSO-D_6 or CDCl_3 - DMSO-D_6 solvent mixtures. ^1H -NMR spectra were obtained using a Varian XL-400 spectrometer operating at 400 MHz at 50°C. The recording conditions for ^1H -NMR were: sample concentration 1% (g/mL), spectral width 4798.5 Hz, acquisition time 1.67 s, pulse delay 5 s, and number of scans 16. The ^{13}C -NMR spectra were obtained with the same spectrometer at 100 MHz at 90°C. The conditions for ^{13}C -NMR measurements were: sample concentration 10% (g/mL), spectral width 20000 Hz, acquisition time 0.4 s, flip

**Figure 4** Kelen-Tudos plot for low-conversion bulk S-AA copolymer.

angle 45° , pulse delay 1.6 s, and number of scans 512. DMSO was used as the locking agent for all NMR spectra.

RESULTS AND DISCUSSION

^1H - and ^{13}C -NMR Spectra of S-AA Copolymer

Figure 1 shows a typical 400 MHz ^1H -NMR spectra of low-conversion S-AA bulk copolymer dissolved in DMSO-D_6 and in $\text{DMSO-D}_6\text{-CDCl}_3$ at 50°C . The chemical shift of different protons respectively are: 1–2 PPM for all methine protons and the methylene proton of the styrene units in the copolymer chain; 2.3 PPM for the methylene proton of the acrylic acid

unit in the copolymer chain; 3.3 PPM for water in DMSO-D_6 , 5.2–6.4 PPM multiplets for the end groups of the copolymer chains that may be double bonds and isobutylnitrile; 6.4–7.4 PPM for aromatic protons; and 12.1 for the proton of the carboxyl group on the copolymer chain.

The resonance behavior of the carboxyl proton is heavily affected by the solvent used. A clear single resonance peak appears in the ^1H -NMR spectra if DMSO-D_6 is used and the baseline is straight. This sharp peak disappears, however, when a $\text{DMSO-D}_6\text{-CDCl}_3$ solvent mixture is used. Such behavior may result from dissociation of the carboxyl proton ion (or carboxylate ion pair) or from the formation of hydrogen bonds with the chlorides in chloroform. As mentioned above, S-AA copolymer having more

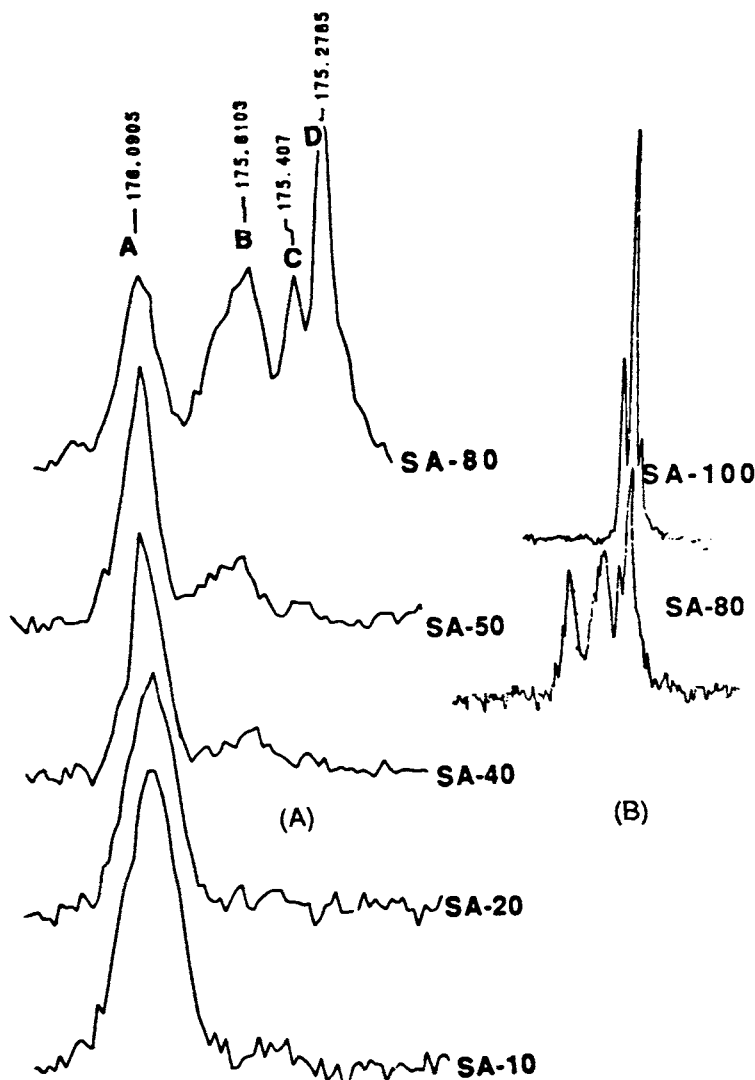


Figure 5 Expanded ^{13}C -NMR spectra of carboxyl carbon on S-AA copolymer. Peak: (A) SAS, (B) AAS, (C) AAA, (D) AAA.

than 60% styrene units cannot be dissolved in DMSO. Hence, samples like SA-20 did not show all proton resonance peaks.

Figure 1 clearly shows that the $^1\text{H-NMR}$ spectrum of S-AA copolymer is very different from that of (methyl) acrylate copolymers that have sequence sensitive peaks caused by the ester groups.^{15,25} $^1\text{H-NMR}$ of S-AA copolymer does not provide the information needed for determination of the sequence distribution.

Figure 2 is an example of the 100 MHz $^{13}\text{C-NMR}$ spectrum of S-AA bulk copolymer in DMSO- D_6 at 90°C. The resonance peak at 44 PPM is produced by the methylene carbon of the acrylic acid unit in the copolymer chain. All other carbons in the copolymer chain in the 36–42 PPM range were overlapped by DMSO. The $\text{C}_2\text{-C}_5$ carbons of phenyl have peaks at 125–130 PPM, the C_1 carbon of phenyl at 143–144.5 PPM (tripeaks), and the carboxyl carbon at 175–177.5 PPM (tripeaks). Two tripeaks caused by carboxyl carbon and C_1 in phenyl may contain the information on the monomer sequence distribution. This will be discussed later.

The smaller peaks are the most interesting part of Figure 2. Higher concentration samples (> 10%) were used in order to facilitate quantitative analysis. However, the noise in the spectra increases with the concentration because the samples cannot be easily dissolved and they have high viscosity. Higher temperatures were tested in order to reduce the affect of noise. The results are shown in Figure 3. The density of sample peaks is enhanced by increasing the temperature. Molecular motion increases allowing individual chain segments to partially average the effect of local magnetic fields. When this occurs, the linewidth narrows and a more well-defined spectra results.³⁶ As indicated in the experimental section, $^{13}\text{C-NMR}$ spectra were recorded at 90°C.

Composition of S-AA Copolymers and Reactivity Ratio of Monomers

$^1\text{H-NMR}$ is a valuable method for the quantitative analysis of copolymer composition. The resonance peak areas of copolymer chain and side groups are usually preferred for composition determinations. In this work, results from $^1\text{H-}$ and $^{13}\text{C-NMR}$ were obtained and compared. Table I lists the initial monomer mole fraction, the final conversions of the bulk copolymerization reactions, and average compositions of the copolymers (mole fraction of styrene) as determined by $^1\text{H-}$ and $^{13}\text{C-NMR}$. The composition results calculated by different methods are listed in Table II, in which the composition

numbers are obtained according to the following equations:

$$F_{S-1} = A_{\text{Ph}} / (5A_{\text{COOH}} + A_{\text{Ph}})$$

$$F_{S-2} = 3A_{\text{Ph}} / 5A_{\text{CHCH}_2}$$

$$F_{S-3} = A_{\text{Ph-1}} / A_{\text{COO}}$$

$$F_{S-4} = A_{\text{Ph-2-5}} / (5A_{\text{COO}} + A_{\text{Ph-2-5}})$$

where F_S is the mole fraction of styrene in the copolymers, and the subscript number in F_{S-n} rep-

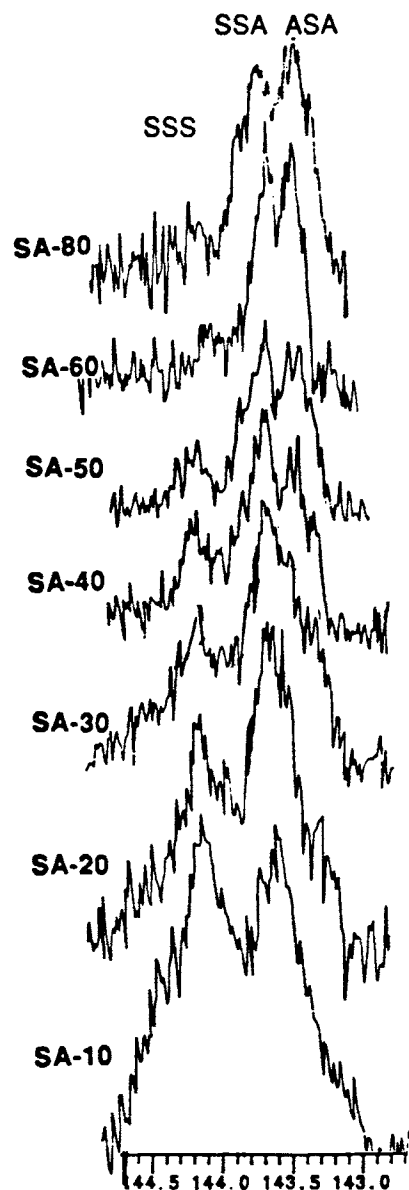


Figure 6 Expanded $^{13}\text{C-NMR}$ spectra of C_1 carbon of phenyl on S-AA copolymers.

represents the quantitative analysis methods; A_{Ph} , A_{COOH} , and A_{CHCH_2} are the 1H -NMR resonance peak areas of protons on phenyl, $-COOH$, and $-CRH-CH_2-$ ($R = COOH$ or phenyl), respectively; A_{Ph-1} , A_{Ph-2-5} , and A_{COO} are the ^{13}C -NMR resonance peak areas of the first carbon, the other five carbons on phenyl, and the carbon on $-COOH$, respectively.

The data in Table II show that the styrene fractions of S-AA copolymers measured by different methods are approximately equal. However, careful analysis shows that the F_{S-2} and F_{S-4} results are relatively higher than those from F_{S-1} and F_{S-3} . One reason for this F_{S-1} result is because the proton resonance peak of $CH(COOH)$ is overlapped by DMSO, in which the overlapped part is calculated into the DMSO peak area. The peak area differences between COO and C_2-C_5 obtained with F_{S-3} method is too large. The more accurate results were obtained from F_{S-2} and F_{S-4} and these values were used for calculation of the monomer reactivity ratios.

The reactivity ratios of monomer can be determined from the feed and low-conversion copolymer compositions by the well-known Kelen-Tudos plot methods.^{32,37} The corresponding Kelen-Tudos plot

for S-AA copolymerization system is shown on Figure 4. The reactivity ratios were calculated from the slope and intercept according to the recommended expression:³⁷

$$\eta = (r_a + r_s/\alpha)\xi - r_s/\alpha$$

where

$$\eta = G/(\alpha + F), \quad \xi = F/(\alpha + F)$$

$$G = [(F_a - F_s)/F_a](f_a/f_s)$$

$$F = (F_a/F_s)(f_a/f_s)^2$$

$$\alpha = (F_{\min}F_{\max})^{1/2}$$

where f_a , f_s , F_a , and F_s , respectively, represent the mole fraction of acrylic acid and styrene in the initial monomer feed and in the low-conversion bulk copolymers. The calculated reactivity ratios of r_a (acrylic acid) and r_s (styrene) were 0.13 and 0.38, respectively, reported in the literature to be $r_a = 0.15$, $r_s = 0.25$.³⁸ The differences may be caused by different determination methods.

Table III Calculated Triads with $r_a = 0.13$, $r_s = 0.38$, and $\alpha = 0.36$

Triad Fraction Centered by Acrylic Acid							
Sample Code	f_a	F_a	P_{AA}	F_{AAA}	F_{AAS}	F_{SAS}	
SA-5	0.071	0.153	0.167	0.000	0.019	0.981	
SA-10	0.138	0.235	0.297	0.000	0.040	0.960	
SA-20	0.265	0.343	0.487	0.002	0.086	0.912	
SA-30	0.382	0.375	0.620	0.006	0.138	0.857	
SA-40	0.491	0.429	0.717	0.012	0.198	0.790	
SA-50	0.591	0.462	0.792	0.025	0.266	0.709	
SA-60	0.684	0.537	0.851	0.048	0.343	0.609	
SA-80	0.853	0.667	0.938	0.184	0.490	0.326	
Triad Fraction Centered by Styrene							
Sample Code	f_s	F_s	P_{SS}	F_{SSS}	F_{SSA}	F_{ASA}	
SA-5	0.929	0.847	0.990	0.694	0.278	0.028	
SA-10	0.862	0.765	0.980	0.494	0.418	0.088	
SA-20	0.735	0.657	0.955	0.263	0.500	0.237	
SA-30	0.618	0.625	0.925	0.145	0.471	0.384	
SA-40	0.509	0.572	0.889	0.080	0.406	0.514	
SA-50	0.409	0.538	0.842	0.043	0.330	0.627	
SA-60	0.316	0.463	0.780	0.022	0.254	0.724	
SA-80	0.147	0.333	0.571	0.004	0.116	0.880	

Sequence Distribution of the Bulk Copolymer

Figure 5 and Figure 6 show the expanded ^{13}C -NMR spectra of the carboxyl carbon and the C_1 carbon of phenyl in the copolymer, respectively. The split resonance peaks for one kind of carbon make it possible to investigate the monomer sequence distribution. The triads were assigned as shown in Figures 5 and 6. Assuming that the AM model^{33,34} is valid for these copolymer systems and that the assignments in Figures 5 and 6 are correct, the fraction of triads measured should be in agreement with those calculated from the AM statistics-kinetics model. According to Bovey's treatment,¹⁴ the AA centered and S centered triads can be given by the following set of equations:

Table IV Acrylic Acid Centered Triad Distribution of S-AA Bulk Copolymers

Sample Code	Fraction of Triads	
	Measured by ^{13}C -NMR	Theory
	F_{SAS}	
SA-5	1.000	0.981
SA-10	0.939	0.960
SA-20	0.927	0.912
SA-30	0.860	0.867
SA-40	0.768	0.790
SA-50	0.668	0.709
SA-60	0.569	0.609
SA-80	0.270	0.326
	F_{AAS}	
SA-5	0.000	0.019
SA-10	0.061	0.040
SA-20	0.073	0.086
SA-30	0.135	0.138
SA-40	0.207	0.198
SA-50	0.269	0.266
SA-60	0.337	0.343
SA-80	0.450	0.490
	F_{AAA}	
SA-5	0.000	0.000
SA-10	0.000	0.000
SA-20	0.000	0.002
SA-30	0.005	0.006
SA-40	0.024	0.012
SA-50	0.063	0.025
SA-60	0.094	0.048
SA-80	0.280	0.184

Table V Styrene Centered Triads Distribution of S-AA Bulk Copolymers

Sample Code	Fraction of Triads	
	Measured by ^{13}C -NMR	Theory
	F_{ASA}	
SA-5	0.014	0.028
SA-10	0.022	0.088
SA-20	0.220	0.238
SA-30	0.346	0.384
SA-40	0.456	0.514
SA-50	0.555	0.627
SA-60	0.619	0.724
SA-80	0.755	0.880
	F_{SSA}	
SA-5	0.264	0.278
SA-10	0.450	0.418
SA-20	0.498	0.500
SA-30	0.471	0.471
SA-40	0.435	0.406
SA-50	0.383	0.329
SA-60	0.284	0.254
SA-80	0.192	0.116
	F_{SSS}	
SA-5	0.731	0.694
SA-10	0.530	0.494
SA-20	0.279	0.263
SA-30	0.183	0.145
SA-40	0.109	0.080
SA-50	0.081	0.043
SA-60	0.078	0.022
SA-80	0.054	0.004

$$F_{\text{AAA}} = (P_{\text{AA}})^2$$

$$F_{\text{AAS}} = F_{\text{SAA}} = 2(P_{\text{AA}})(1 - P_{\text{AA}})$$

$$F_{\text{SAS}} = (1 - P_{\text{AA}})^2$$

$$F_{\text{SSS}} = (P_{\text{SS}})^2$$

$$F_{\text{SSA}} = F_{\text{ASS}} = 2(P_{\text{SS}})(1 - P_{\text{SS}})$$

$$F_{\text{ASA}} = (1 - P_{\text{SS}})^2$$

where $P_{\text{AA}} = r_a f_a / (1 - f_a + r_a f_a)$, $P_{\text{SS}} = r_s f_s / (1 - f_s + r_s f_s)$ and P_{AA} (or P_{SS}) is the probability that acrylic acid (or styrene) will add to a growing chain ending in acrylic acid (or styrene), f_a and f_s are the mole fractions of acrylic acid and styrene in the feed,

F_{AAA} , F_{AAS} , and F_{SAS} represent the AA centered triad fractions; F_{SSS} , F_{SSA} , and F_{ASA} are the S centered triad fractions. The calculated results of triads with $r_a = 0.13$, $r_s = 0.38$, and $\alpha = 0.36$ are listed in Table III. The experimental results of normalized triad fractions are compared with theoretical results in Tables IV and V. The experimental results for AA centered triads are almost the same as those determined from statistics. The values measured for S centered triads are also in very good agreement with the calculated results even though the tripeak of C_1

resonance is not split completely. These results indicate the assignments in Figures 5 and 6 are correct.

Figure 5 shows that the resonance peaks of carboxyl carbon not only exhibit three main peaks, but also every peak splits into other tripeaks. This becomes clearer for the SA-80 copolymer and the SA-100 homopolymer. The further resonance phenomenon may be caused by the different configuration of copolymer segments (coisotacticity).^{17,18} Unfortunately, these splits are too small to analyze quantitatively.

Table VI Triad Distributions of Emulsion Copolymers (SA-E-*n*) and Their Composition at Different Conversions and for the Corresponding Bulk Copolymers (SA-B-*n*) at Low Conversion

Sample Code	Conversion (%)	Fraction of Styrene in Polymer (%)	Triad Fractions Centered by Styrene		
			F_{SSS}	F_{SSA}	F_{ASA}
SA-E-40	5	0.748	0.625	0.348	0.026
	7	0.713	0.582	0.373	0.045
	11	0.732	0.521	0.366	0.113
	50	0.710	0.472	0.408	0.120
SA-B-40	4	0.527	0.109	0.435	0.456
SA-E-30	12	0.758	0.655	0.339	0.006
	18	0.774	0.646	0.342	0.012
	25	0.786	0.642	0.335	0.023
	65	0.781	0.624	0.360	0.016
SA-B-30	3	0.625	0.183	0.471	0.345
SA-E-20	6	0.763	0.668	0.316	0.016
	17	0.800	0.633	0.294	0.028
	52	0.806	0.718	0.271	0.011
	78	0.813	0.715	0.260	0.025
SA-B-20	2	0.657	0.282	0.498	0.220
			Triad Fractions Centered by Acrylic Acid		
			F_{AAA}	F_{AAS}	F_{SAS}
SA-E-40	5	0.748	0.064	0.206	0.730
	7	0.713	0.066	0.180	0.754
	11	0.732	0.051	0.173	0.776
	50	0.710	0.055	0.181	0.764
SA-B-40	4	0.572	0.024	0.207	0.768
SA-E-30	12	0.758	0.000	0.072	0.928
	18	0.774	0.000	0.067	0.933
	25	0.786	0.000	0.072	0.928
	65	0.781	0.043	0.045	0.912
SA-B-30	3	0.625	0.005	0.135	0.860
SA-E-20	6	0.763	0.017	0.121	0.863
	17	0.800	0.046	0.130	0.824
	52	0.806	0.000	0.130	0.870
	78	0.813	0.000	0.135	0.865
SA-B-20	2	0.657	0.000	0.073	0.927

Sequence Distribution of Emulsion Copolymer

Table VI lists the triad fractions and composition of three emulsion copolymers at different conversions and of the corresponding bulk copolymers at low conversion. The data in Table VI show that F_{SSS} decreases and F_{ASA} increases as conversion increases. This fact becomes clearer when the acrylic acid content is higher (SA-E-30 or -40). The change of all triads and of composition with conversion is not great at conversions less than 80%. With the emulsion copolymers, F_{SSS} is much smaller and F_{ASA} much higher than the corresponding F_{SSS} and F_{ASA} values for bulk copolymers. Hence more styrene homopolymer is formed in emulsion S-AA copolymerization. The overall concentration of acrylic acid becomes higher as the conversion increases. The reactivity ratio measured by bulk copolymer cannot be used to predict the intramolecular structure in the complex emulsion copolymerization system. Table VI also shows that the AA-centered triad fractions of emulsion copolymers are similar to those of bulk copolymers.

Polymerization in emulsion systems takes place mainly in the micelles or in the polymer particles where the hydrophobic monomers are primarily located.³⁹ The oligomer radicals, which can precipitate or be captured by micelles or polymer particles, are produced in the water phase when water-soluble initiators are employed and these oligomers may grow significantly in the water phase when hydrophilic monomers are used.⁴⁰ Thus for the hydrophilic/hydrophobic system of this study one would expect that in the first stage of copolymerization, large radical oligomers formed in the water would be comprised mainly of water-soluble monomers. If this were true, the F_{AAA} values of emulsion copolymers should be much higher than those of the bulk copolymers. In fact, the experimental results do not agree with this supposition even when high acrylic acid concentrations are used in the feed. In this case, if the conversion is not too high (significant styrene exists), the radical oligomers may grow to a definite size (the radical oligomer size is greater than 2–3 but not too large)⁴¹ and enter the micelles or polymer particles to continue propagation. Because of the high content of hydrophobic monomer, styrene, in the micelles and polymer particles, more homopolymer (large F_{SSS}) will be produced. These data indicate that the major loci of polymerization remain in the micelles and/or particles even with high AA concentration. Much more work is needed to understand the details of the reactions in the water phase and their impact on copolymer characteristics.

CONCLUSIONS

The sequence distribution of styrene-acrylic acid copolymers can be measured by ¹³C-NMR of the carboxyl carbon and the C₁ carbon of phenyl in S-AA copolymers. Low-conversion copolymer composition data obtained by NMR at different initial monomer ratios were used with the Kelen-Todos plot method to determine the reactivity ratios of $r_a = 0.13$ and $r_s = 0.38$. The resonance peaks split by triads were assigned and confirmed by comparing experimental triad values with those calculated from the Alfrey-Mayo statistics-kinetics model. The triad distribution of S-AA emulsion copolymers were measured in an effort to obtain more information about emulsion copolymerization mechanisms when hydrophilic/hydrophobic monomers are used.

The authors are indebted to Dr. Leslie T. Gelbaum for running the NMR equipment and to Mr. Pei-Hua Yang for the assistance in experiments. The authors also appreciate the financial support of the National Science Foundation under Grant CTS-9023240. The U.S. Government has certain rights to patents in this material.

REFERENCES

1. R. Yocum and E. Nyquist, *Functional Monomers: Their Preparation, Polymerization and Application*, Marcel Dekker, New York, 1973.
2. R. L. Schild, M. S. El-Aasser, G. W. Poehlein, and J. W. Vanderhoff, in *Emulsions, Latices and Dispersions*, P. Becker and M. N. Yudenfreund, Eds., Marcel Dekker, New York, 1978, p. 99.
3. S. Juang and I. M. Krieger, *J. Polym. Sci. Polym. Chem. Ed.*, **14**, 2089 (1976).
4. D. A. Upson, *J. Polym. Sci. Polym. Symp.*, **72**, 45 (1985).
5. J. L. Guillaume, C. Pichot, and J. Guillot, *J. Polym. Sci. Polym. Chem. Ed.*, **26**, 1937 (1988).
6. G. L. Shoaf, *Emulsion Copolymerization with Carboxylic Acids*, Ph.D. dissertation, Georgia Institute of Technology, 1989.
7. G. L. Shoaf and G. W. Poehlein, *Ind. Eng. Chem. Res.*, **29**, 1701 (1990).
8. D. M. Lange, *Emulsion Copolymerization with Functional Monomers in Continuous Reactors*, Ph.D. dissertation, Georgia Institute of Technology, 1991.
9. F. A. Bovey, *High Resolution NMR of Macromolecules*, Academic, New York, 1972.
10. J. C. Randall, *Polymer Sequence Determination, Carbon-13 NMR Method*, Academic, New York, 1977.
11. J. R. Ebdon, in *Development in Polymer Characterization*, J. V. Dawkins, Ed., New York, 1980, Vol. 2, Applied Science, pp. 1–29.

12. J. L. Koenig, *Chemical Microstructure of Polymer Chains*, Wiley-Interscience, New York, 1980.
13. H. N. Cheng, in *Modern Methods of Polymer Characterization*, H. G. Barth and J. W. Mays, Eds., John Wiley & Sons, Inc., New York, 1991, pp. 409-493.
14. F. A. Bovey, *J. Polym. Sci.*, **62**, 197 (1962).
15. K. Ito, Y. Yamashita, *Polym. Letters*, **3**, 625 (1965).
16. K. Ito, S. Iwase, K. Umehara, and Y. Yamashita, *J. Macromol. Sci. (Chem.)*, **A1**(5), 891 (1967).
17. K. Ito and Y. Yamashita, *Polym. Letters*, **3**, 631 (1965).
18. K. Ito and Y. Yamashita, *J. Polym. Sci., B6, Polym. Letters*, **6**, 227 (1968).
19. A. Simmons, A. Natansohn, and A. Eisenberg, *J. Polym. Sci. A, Polym. Chem.*, **25**, 2221 (1987).
20. T. Hayashi, Y. Inoue, and R. Chujo, *Macromolecules*, **21**, 3139 (1988).
21. H. N. Cheng, and G. H. Lee, *Macromolecules*, **21**, 3164 (1988).
22. H. Sato, T. Ishikawa, K. Takebayashi, and Y. Tanaka, *Macromolecules*, **22**, 1748 (1989).
23. H. Ketel, J. Beulen, and G. van der Velden, *Macromolecules*, **21**, 2032 (1988).
24. R. Volpe and T. E. Hogen-Esch, *Macromolecules*, **23**, 4196 (1990).
25. F. Heatley, G. Yu, W. Sun, E. J. Pywell, R. H. Mobbs, and C. Booth, *Polym. J.*, **26**, 583 (1990).
26. J. J. Uebel and F. J. Dinan, *J. Polym. Sci. Polym. Chem. Ed.*, **21**, 1773 (1983); **21**, 2427 (1983).
27. L. T. Kale, K. F. O'Driscoll, F. J. Dinan, and J. J. Uebel, *J. Polym. Sci. Polym. Chem. Ed.*, **24**, 3145 (1986).
28. A. S. Brar and A. K. Saini, *J. Appl. Polym. Sci.*, **32**, 4607 (1986).
29. A. S. Brar, G. S. Kapur, and S. K. Dubey, *Eur. Polym. J.*, **20**, 371 (1988).
30. A. S. Brar and G. S. Kapur, *Polym. J.*, **20**, 371 (1988); **20**, 811 (1988).
31. A. S. Brar, E. Aranan, and G. S. Kapur, *Polym. J.*, **21**, 689 (1989).
32. J. C. J. F. Tacx, G. P. van der Velden, and A. L. German, *J. Polym. Sci. A, Polym. Chem.*, **26**, 1439 (1988).
33. J. C. J. F. Tacx, G. P. van der Velden, and A. L. German, *Polymer*, **29**, 1675 (1988).
34. G. H. J. van Doremaele, A. L. German, N. K. de Vries, and G. P. M. Van der Velden, *Macromolecules*, **23**, 4206 (1990).
35. D. Murry and I. Piirma, International Polymer Colloid Group Newsletter, September, 1991.
36. P. J. Tarcha, R. M. Fitch, and L. W. Jelinski, in *Science and Technology of Polymer Colloids*, Vol. II, G. W. Poehlein, R. H. Ottewill and J. W. Goodwin, Eds., Martinus Nijhoff Publishers, New York, 1983, p. 589.
37. T. Kelen and F. Tudos, *J. Macromol. Sci.-Chem.*, **A9**, 1 (1975).
38. V. R. Kerber, *Makrom. Chem.*, **96**, 30 (1966).
39. W. V. Smith and R. H. Ewart, *J. Chem. Phys.*, **16**, 592 (1948).
40. R. M. Fitch and C. H. Tsai, in *Polymer Colloids*, R. M. Fitch, Ed., Plenum Press, New York, 1971, pp. 73, 103.
41. I. A. Maxwell, B. R. Morrison, D. H. Napper, and R. G. Gilbert, *Macromolecules*, **24**, 1629 (1991).

Received September 21, 1992

Accepted November 13, 1992